SUPPLEMENTARY INFORMATION TO THE MANUSCRIPT

Effect of yttrium Content in the $La_{2-x}Y_xMgNi_9$ Battery Anode Alloys on the Structural, Hydrogen Storage and Electrochemical Properties

ChuBin Wan [a, b], R.V. Denys [b, c] and V.A.Yartys [b] *

[a] University of Science and Technology Beijing, 100083, China
[b] Institute for Energy Technology, P.O. Box 40, Kjeller NO-2027, Norway
[c] HYSTORSYS AS, P.O. Box 45, Kjeller NO-2027, Norway

Table S1.

Atomic parameters for $La_{1.75}Y_{0.25}MgNi_9$ compound ($PuNi_3$-type).

Atom	Wyckoff site	*x/a*	*y/b*	*z/c*	Occupancy
(La/Y)1	3a	0	0	0	0.96(1)/0.04(1)
(La/Y/Mg)2	6c	0	0	0.1465(1)	0.40(1)/0.10(1)/0.5(-)
Ni1	3b	0	0	1/2	1.0(-)
Ni2	6c	0	0	0.3270(2)	1.0(-)
Ni3	18h	0.4986(4)	-x	0.0826(1)	1.0(-)

U_{iso} for all atoms is set to 0.01 Å^2 and not refined.

Table S2.

Atomic parameters for $La_{1.5}Y_{0.5}MgNi_9$ compound ($PuNi_3$-type).

Atom	Wyckoff site	*x/a*	*y/b*	*z/c*	Occupancy
(La/Y)1	3a	0	0	0	0.81(2)/0.19(2)
(La/Y/Mg)2	6c	0	0	0.1491(2)	0.34(1)/0.16(1)/0.5(-)
Ni1	3b	0	0	1/2	1.0(-)
Ni2	6c	0	0	0.3289(2)	1.0(-)
Ni3	18h	0.4976(4)	-x	0.0829(2)	1.0(-)

U_{iso} for all atoms is set to 0.01 Å^2 and not refined.

Table S3.

Atomic parameters for $La_{1.25}Y_{0.75}MgNi_9$ compound ($PuNi_3$-type).

Atom	Wyckoff site	*x/a*	*y/b*	*z/c*	Occupancy
(La/Y)1	3a	0	0	0	0.726(5)/0.274(5)
(La/Y/Mg)2	6c	0	0	0.1430(1)	0.276(6)/0.233(6)/0.5(-)
Ni1	3b	0	0	1/2	1.0(-)
Ni2	6c	0	0	0.3325(1)	1.0(-)
Ni3	18h	0.5008(3)	-x	0.0836(1)	1.0(-)

U_{iso} for all atoms is set to 0.01 Å^2 and not refined.

Table S4.

Crystallographic data for $La_{2.25}Y_{0.75}MgNi_{14}D_{18}$ from Rietveld refinement of NPD data.

Space group $R\bar{3}m$; a = 5.3762(9) Å, c = 39.41(1) Å, V = 986.4(4) Å^3.

Atom	Wyckoff site	*x*/*a*	*y*/*b*	*z*/*c*	U_{iso} (Å^2)	Occupancy
(La/Y)1	6*c*	0	0	0.043(–)	0.01	0.75/0.25(–)
(La/Y)2/Mg	6*c*	0	0	0.153(–)	0.01	0.375/0.125/0.5(–)
Ni1	18*h*	0.507(–)	-x	0.110(–)	0.01	1.0(–)
Ni2	9*e*	0.5	0	0	0.01	1.0(–)
Ni3	6*c*	0	0	0.277(–)	0.01	1.0(–)
Ni4	6*c*	0	0	0.392(–)	0.01	1.0(–)
Ni5	3*b*	0	0	0.5	0.01	1.0(–)
D1	6*c*	0	0	0.316(–)	0.02	0.37(–)
D2	18*h*	0.499(–)	-x	0.046(–)	0.02	0.75(–)
D3	18*h*	0.157(–)	-x	0.110(–)	0.02	0.49(–)
D4	6*c*	0	0	0.345(–)	0.02	0.45(–)
D5	18*h*	0.849(–)	-x	0.100(–)	0.02	0.48(–)
D6	6*c*	0	0	0.205(–)	0.02	0.48(–)
D7	18*h*	0.908(–)	-x	0.197(–)	0.02	0.27(–)
D8	6*c*	0	0	0.456(–)	0.02	0.47(–)
D9	18*h*	0.491(–)	-x	0.149(–)	0.02	0.46(–)

Table S5.

Interatomic distances and sites of occupied interstices in structure of $La_{1.5}Y_{0.5}MgNi_9D_{12.4}$ and $La_2MgNi_9D_{13}$ [1].

	$La_{1.5}Y_{0.5}MgNi_9D_{12.4}$			**$La_2MgNi_9D_{13}$ [1]**		
Slab	Atoms	Distance[a] (Å)	Interstitial site	Atoms	Distance[a] (Å)	Interstitial site
$RENi_5$	D1…RE1 D1…Ni2 D1…Ni2 D1…Ni3 D1…D1 D1…D2 D1…D3	2.54(1) 1.62(2) 1.67(2) 1.75(1) 0.38(3) 0.97(2) 1.04(3)	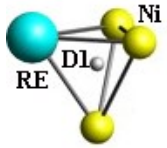 Tetrahedron $RENi_3$	D1…2 La1 D1…Ni2 D1…Ni2 D1…Ni3 D1…D1 D1…D2	2.758(2) 1.62(2) 1.68(2) 1.69(1) 1.05(2) 1.79(2)	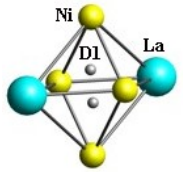 Tetragonal pyramid La_2Ni_3
	D2…Ni2 D2…3 Ni3 D2…6 D1 D2…3 D3	1.55(4) 1.74(2) 1.75(3) 1.77(4)	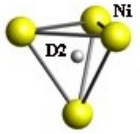 Tetrahedron Ni_4	D2…Ni2 D2…3 Ni3 D2…3 D1 D2…3 D3 D2…D8	1.57(3) 1.69(1) 1.79(2) 1.92(3) 1.42(3)	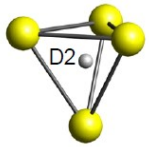 Tetrahedron Ni_4
Interslab Boundary	D3…RE1 D3…Mg/RE2 D3…2 Ni3 D3…D2 D3…2 D4 D3…2 D6 D3…D8	2.77(3) 2.19(3) 1.54(2) 1.77(4) 1.56(2) 1.70(2) 1.61(4)	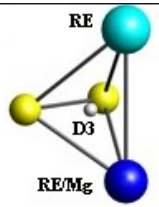 Tetrahedron RE_2Ni_2	D3…La1 D3…Mg/La2 D3…2 Ni3 D3…D2 D3…2 D4 D3…2 D6 D3…D8	2.61(3) 2.15(3) 1.66(2) 1.92(3) 1.36(1) 1.93(2) 1.90(4)	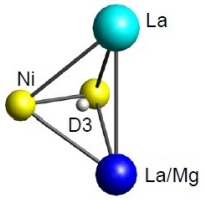 Tetrahedron $La(La/Mg)Ni_2$
	D4…RE1 D4…Mg/RE2 D4…2 Ni3 D4…2 D3 D4…D6	2.44(2) 2.39(1) 1.619(7) 1.56(2) 0.69(2)	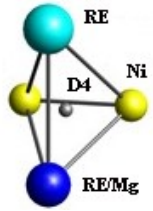 Tetrahedron RE_2Ni_2	D4…La1 D4…Mg/La2 D4…2 Ni3 D4…2 D3 D4…D6 D4…D7	2.62(1) 2.15(1) 1.68(1) 1.36(1) 1.07(2) 1.80(2)	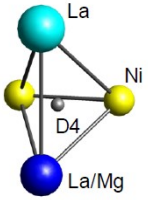 Tetrahedron $La(La/Mg)Ni_2$

REMgNi$_4$	D5…3 Mg/RE2 D5…Ni1 D5…Ni3 D5…2 D6 D5…D8	1.92(1) 1.686(8) 1.591(8) 1.90(2) 1.89(2)	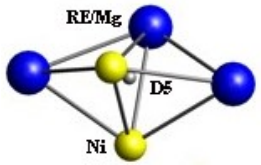 Trigonal bipyramid (RE/Mg)$_3$Ni$_2$	D5…2 Mg/La2 D5…Mg/La2 D5…Ni1 D5…Ni3 D5…2 D5 D5…2 D6 D5…D8	2.711(1) 1.97(1) 1.52(1) 1.74(1) 1.73(1) 1.70(1) 1.77(1)	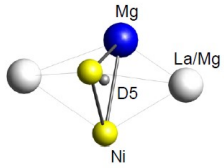 Trigonal pyramid (La/Mg)$_3$Ni$_2$
	D6…Mg/RE2 D6…Mg/RE2 D6…2 Ni3 D6…2 D3 D6…D4 D6…2 D5	2.17(2) 2.76(2) **1.500(9)** 1.70(2) 0.69(2) 1.90(2)	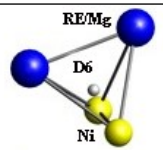 Tetrahedron RE$_2$Ni$_2$	D6…Mg/La2 D6…Mg/La2 D6…2 Ni3 D6…2 D3 D6…D4 D6…2 D5 D6…D7	2.03(1) 2.17(3) 1.73(1) 1.93(2) 1.07(2) 1.70(1) 1.34(4)	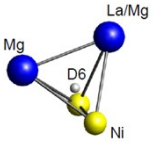 Tetrahedron MgLaNi$_2$
	vacant	vacant	vacant	D7…Mg/La2 D7…3 Ni3 D7…3 D4 D7…3 D6	2.33(9) 1.65(2) 1.80(2) 1.34(4)	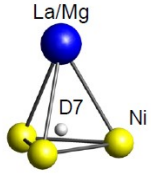 Tetrahedron (La/Mg)Ni$_3$
	D8…Ni1 D8…3 Ni3 D8…D2 D8…3 D3 D8…3 D5	1.62(2) 1.63(1) 1.38(4) 1.61(4) 1.89(2)	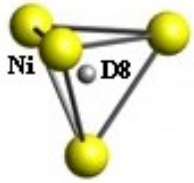 Tetrahedron Ni$_4$	D8…Ni1 D8…3 Ni3 D8…D2 D8…3 D3 D8…3 D5	1.52(1) 1.685(6) 1.42(3) 1.90(4) 1.77(1)	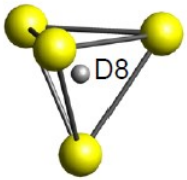 Tetrahedron Ni$_4$

La and Y are labelled as RE (rare earth metals) in in structure of $La_{1.5}Y_{0.5}MgNi_9D_{12.4}$. [a] Table provides the values of the shortest distances between neighboring D sites (1.0–1.9 Å). Such D sites are never simultaneously filled; minimum distance between the neighboring D atoms in the structure exceeds 2 Å.

[1] R.V. Denys, V.A. Yartys, C.J. Webb, Hydrogen in $La_2MgNi_9D_{13}$: The Role of Magnesium, lnorg. Chem., 51 (2012) 4231-4238.

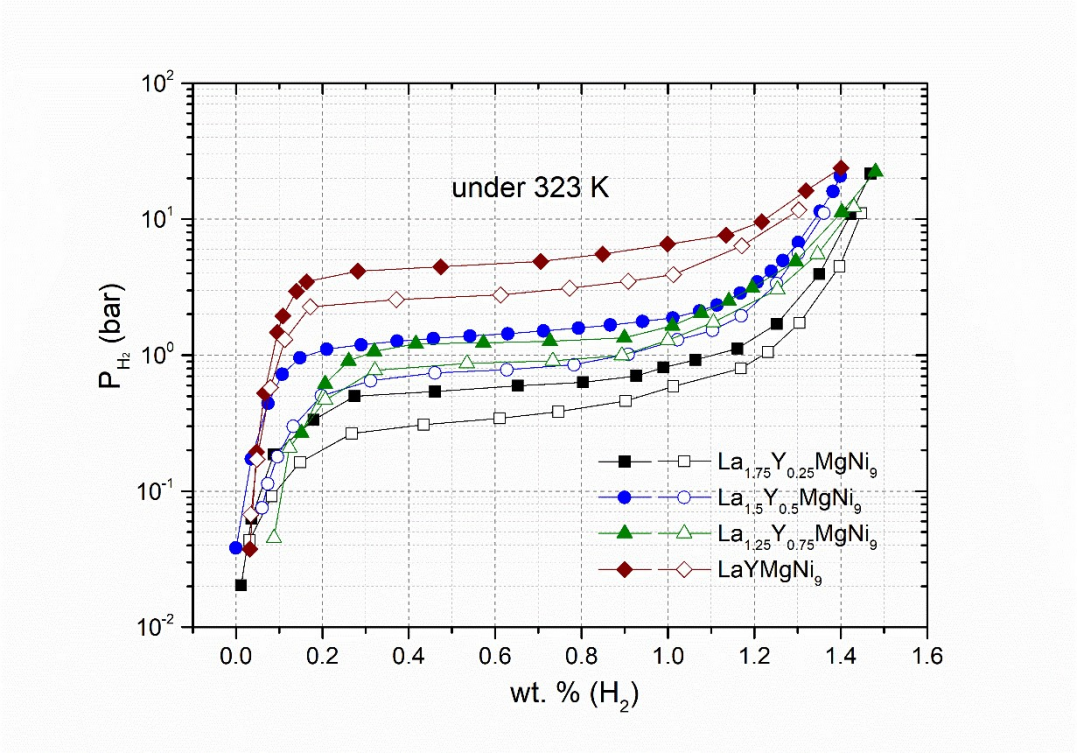

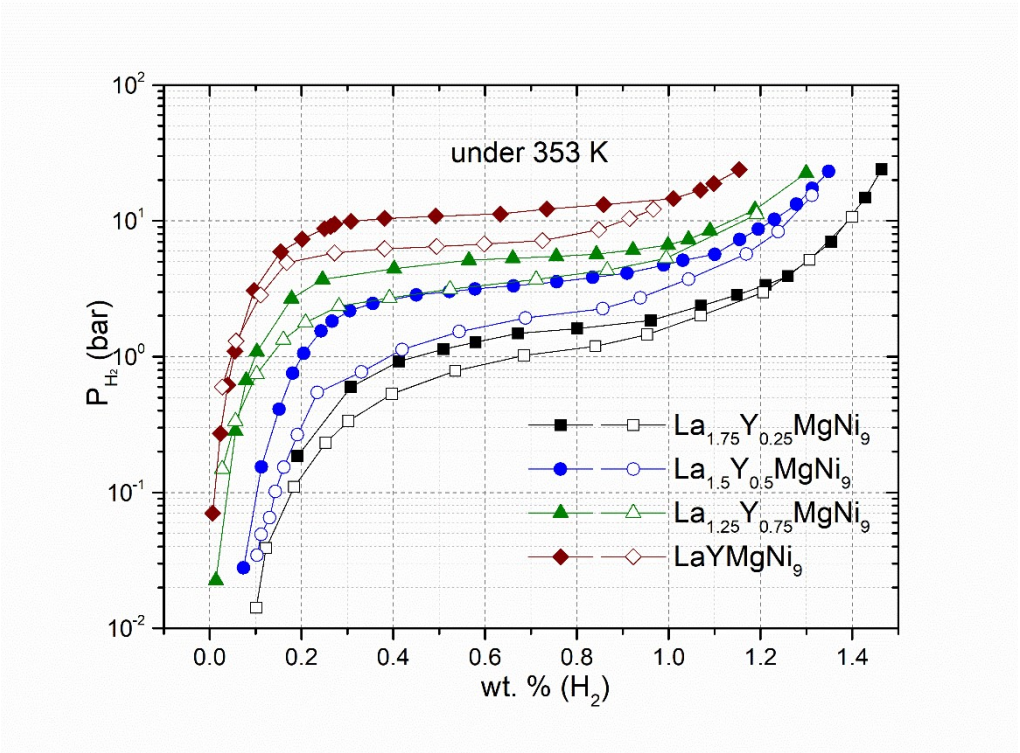

Fig. S1. Absorption-desorption isotherms measured for the $La_{2-x}Y_xMgNi_9$-H_2 system at 50°C and 80°C. Absorption: filled symbols; Desorption: open symbols.

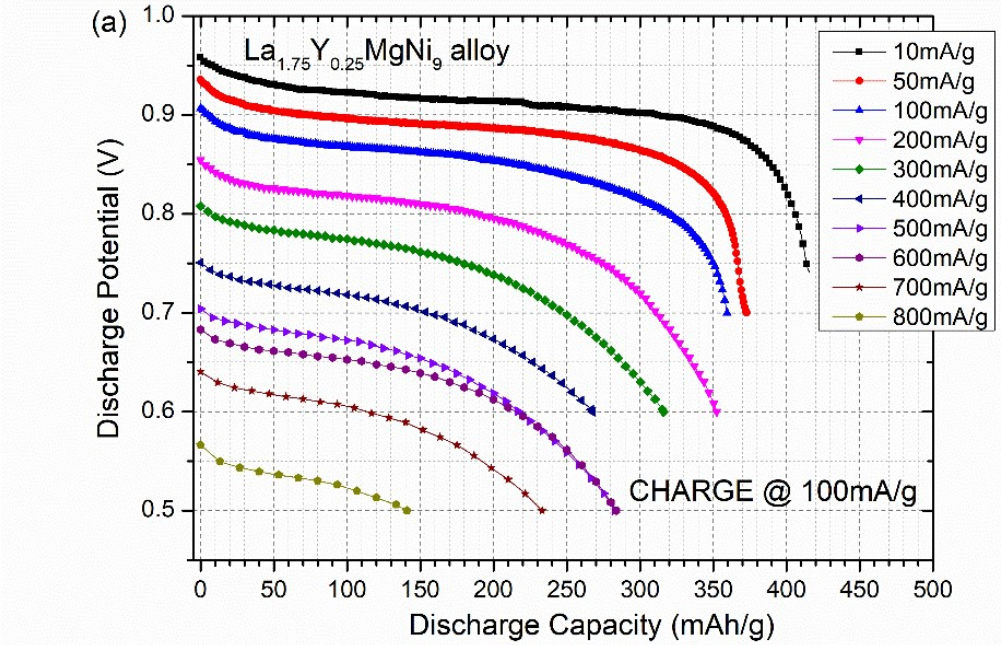
(a)
La1.75Y0.25MgNi9 alloy
10mA/g
50mA/g
100mA/g
200mA/g
300mA/g
400mA/g
500mA/g
600mA/g
700mA/g
800mA/g
CHARGE @ 100mA/g
Discharge Potential (V)
Discharge Capacity (mAh/g)
1.0
0.9
0.8
0.7
0.6
0.5
0
50
100
150
200
250
300
350
400
450
500

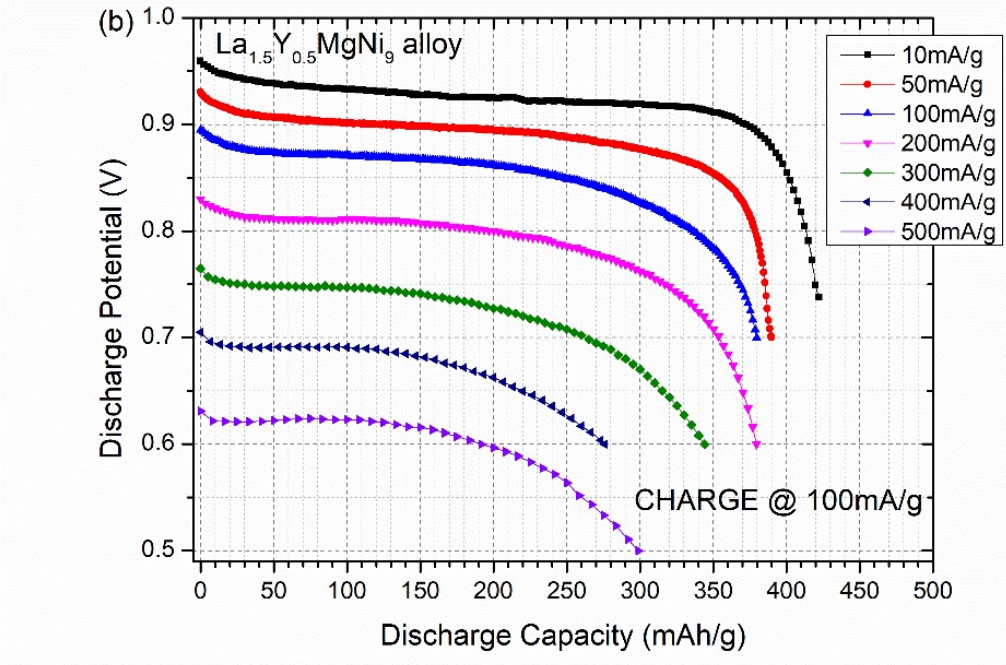
(b)
La1.5Y0.5MgNi9 alloy
10mA/g
50mA/g
100mA/g
200mA/g
300mA/g
400mA/g
500mA/g
CHARGE @ 100mA/g
Discharge Potential (V)
Discharge Capacity (mAh/g)
1.0
0.9
0.8
0.7
0.6
0.5
0
50
100
150
200
250
300
350
400
450
500

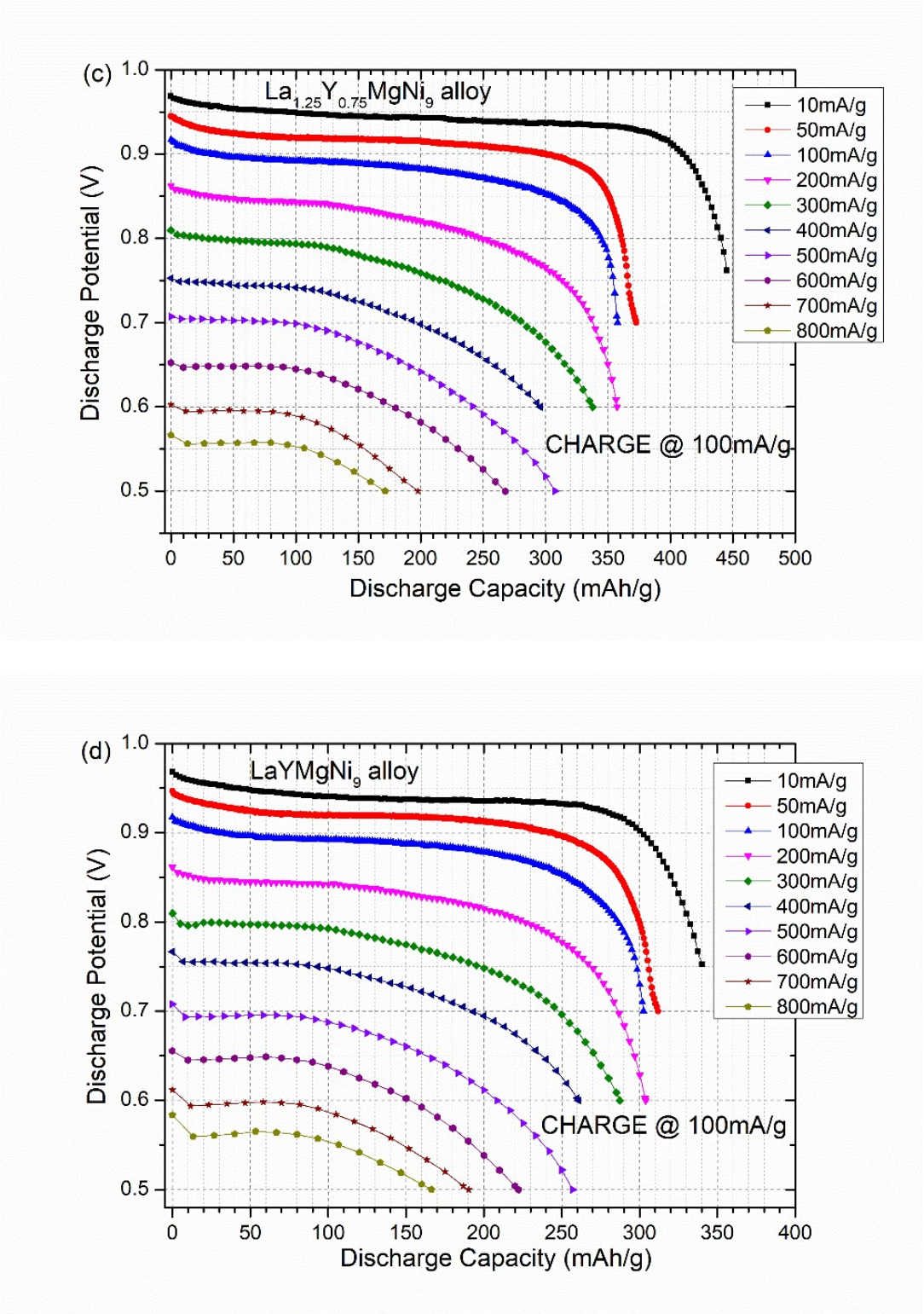

Fig. S2. Discharge capacities of the $La_{2-x}Y_xMgNi_9$ alloy electrodes as a function of applied current densities. All electrodes were charged at a current density of 100 mA/g before the discharge experiments.